Cool Stars, Stellar Systems and the Sun
ASP Conference Series, Vol. 154, 1998
eds. R. A. Donahue and J. A. Bookbinder

The Variable Spectrum of the Yellow Hypergiant ρ Cassiopeiae

G. Israelian[1], A. Lobel[2], C. de Jager[3], and F. Musaev[4]

Abstract:

We have analyzed high-resolution optical spectra of the cool hypergiant ρ Cas covering a period 2 years. The aim of this analysis is to check the range of the effective temperature variations with the pulsation of the atmosphere, in order to study variable emission components in Hα, to investigate the splitting of metallic absorption lines and to compute abundances of Na, Fe and other elements. We found an upper range of $\Delta T_{\rm eff} \simeq 750$ K over a period 17 months, whereas the effective temperature change within a single pulsation period remained limited to 400 K.

We discuss the notorious splitting of low excitation metallic absorption lines observed for ρ Cas. The allowed emission reversals in the cores of these low energy lines emerge from cool and static shells in a bipolar stellar wind. Furthermore, variable absorption in the supersonic stellar wind recurrently produces far violet extended line wings with the atmospherical pulsations, from which we have derived the mass-loss rate and wind extension above the photosphere.

The emission components of Hα suggest the presence of a thermally excited outer atmospherical region (a variable quasi-chromosphere). Several observed parameters (like the mass-loss rate) can be derived theoretically if we assume that the observed "microturbulent" line broadening is not caused by stochastic small-scale turbulent motions (the classical notion of microturbulence) but by thermal motions in stochastically distributed high-temperature sheets behind the many shocks.

1. Introduction

The star ρ Cas is the prototype object of the *hypergiants*. Hypergiants, initially called super-supergiants (Feast & Thackeray 1956) are, according to Keenan's spectral criterion (1971) supergiants with Hα in emission. An additional criterion is that the Fraunhofer lines are significantly broader than those of normal supergiants (de Jager 1998, quoting Smolinski). This spectral definition has two implications, the first being that hypergiants need not always be the brightest stars of their spectral class and there are indeed a few Ia-type supergiants that are brigher than some Ia$^+$-type stars of similar spectral class. The second im-

[1]Instituto de Astrofisica de Canarias, 38200 La Laguna, Tenerife, Canary Islands, Spain
[2]Astronomy Group, Vrije Universiteit Brussel, Pleinlaan 2, B-1050 Brussels, Belgium
[3]SRON Laboratory for Space Research, Sorbonnelaan 2, 3584 CA Utrecht, The Netherlands
[4]Special Astrophysical Observatory, Russian Academy of Sciences, Nizhnii Arkhyz, Stavropolskii Kraii, 357147, Russia

plication is the physical relationship between strongly broadened spectral lines and the occurrence of extended envelopes which implies enhanced mass loss. The answer must most probably be sought in pulsation-driven enhancement of the rate of mass loss. The Hertzsprung-Russell diagram for stars with luminosities above $\log(L/L_{\odot})\simeq 5.3$ contains three kinds of objects: the *hypergiants*, the normal *supergiants* and the *luminous blue variables*(LBVs).

The $T_{\rm eff}$-values of some yellow hypergiants have varied in the last half century. This property seems to be related to the proposed existence of a region of atmospheric instability, the "Yellow Void" drawn in the diagram by thin lines. The Void is a region (Nieuwenhuijzen & de Jager 1995) where the stellar atmospheres are somewhat unstable. There are indications that post-red supergiants evolving along a blueward loop in the HR diagram, undergo enhanced mass loss when approaching the border of the Void (de Jager & Nieuwenhuijzen 1997), at which time they develop into yellow hypergiants. The star ρ Cas has recently been the subject of several investigations. Its chemical abundances were studied by various authors, lately by Takeda & Takada-Hidai (1994) who found from their Na-enhancement that it must be a post-red object. Lobel et al. (1994) studied its pulsation during the period around 1970 and found that ρ Cas is not pulsating radially. The spectral variability during the period November 1993 through December 1995 was described by Lobel et al. (1998). They found that during part of the pulsation periods of enhanced mass loss occur. In order to study the many interesting properties of this object it is being monitored spectroscopically at the La Palma Northern Observatory (Roque de los Muchachos) since 1993, and at the Special Astrophysical Observatory (SAO; Caucuses) since 1995. The monitoring has been intensified recently and since summer 1995 nearly monthly a high-resolution spectrum is being obtained. In this paper we describe some results from this monitoring program.

2. What Are We Investigating?

We have obtained between 1993–95 high-resolution (R=36,000 to 80,000) and high S/N optical spectra of ρ Cas with the UES on WHT (La Palma) and CES (SAO). The chief problems we address are:

1. To check the range of the variations of $T_{\rm eff}$ with the atmospherical pulsation.

2. To understand the physical nature of the splitting of the cores of metallic absorption lines.

3. To find the mechanism(s) causing the intensity and radial velocity of the Hα line core to vary in anti-phase with single metallic lines. Also, why do the Hα line wings turn mutually into emission?

4. To understand the wind driving mechanism of this cool object.

5. To investigate the evolutionary status of this peculiar super-supergiant star.

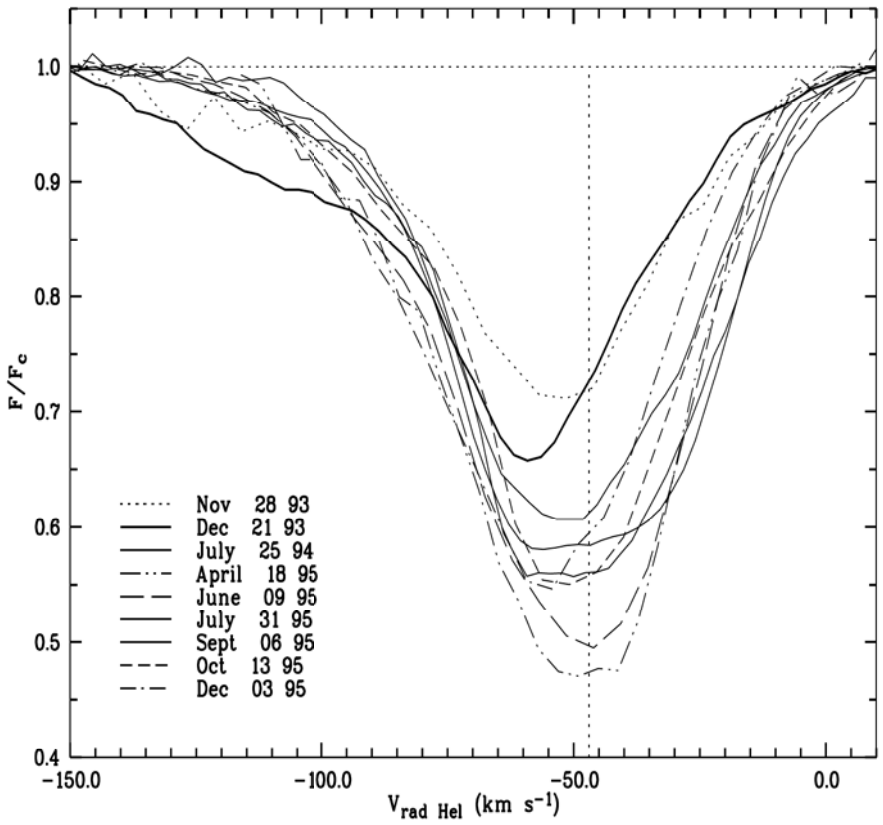

Figure 1. Profile changes of the subordinate Fe I 5572.841 Å line caused by atmospherical pulsation.

3. The Atmospherical Pulsations

We have analyzed 9 optical spectra of ρ Cas covering a period of 2 years. Figure 1 shows the evolution of the unblended Fe I 5572.841 Å line. The velocity scale is heliocentric and the dotted vertical line is drawn at the center-of-mass velocity. Notice the broadening and weakening from the longwave side of the core profile. When the line core assumes maximum depression it becomes nearly symmetric and centers around the systemic velocity (in the phase of minimum $T_{\rm eff}$), whereas the lines become weakest showing a rather triangular profile shape where the line bisector appears blue-shifted with respect to the stellar velocity (view the MPEG movie on the companion CD–ROM for a simulation of its evolution with pulsation). In Fig. 2 we show the changes of the equivalent line widths resulting from the atmospherical pulsation of ρ Cas. The three neutral iron lines at 5569 Å, 5572 Å and 5576 Å belong to the same multiplet. The

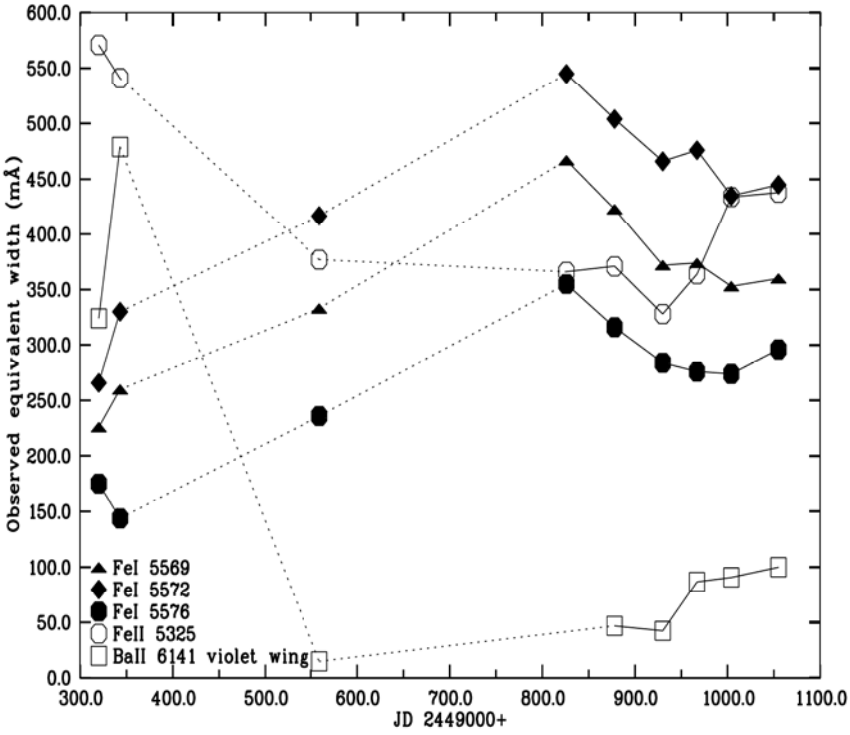

Figure 2. The pulsation modifies the iron ionization equilibrium which causes opposite changes of the equivalent width values of neutral and ionic absorption lines. These changes correspond to a decrease of $T_{\rm eff}$ by ∼400 K between April and Dec. '95

observed increases of $W_{\rm eq}$ by about 200 mÅ between Dec. '93 and April '95 correspond with a decrease of $T_{\rm eff}$ by 750 K, from 7250 K to 6500 K. The latter values have been derived by best atmospherical model fits of the equivalent width values measured from 23 FeI lines and 11 FeII unblended absorption lines. The detection of hidden blends in selected candidate lines was carried out by means of synthetic spectrum calculations. The subsequent decrease of $W_{\rm eq}$ by about 100 mÅ in Fig. 2 corresponds therefore with an increase of $T_{\rm eff}$ by about 400 K in a single pulsation cycle. The opposite variation of the neutral and ionic lines results from a displacement of the ionization equilibrium during the atmospherical pulsations. The changes of $T_{\rm eff}$ vary around $T_{\rm eff}\simeq$7000 K which changes the thermal conditions in the line formation region.

The Hα profile is certainly filled in by emission, which affects the $V_{\rm rad}$ values measured by us. A contribution of emission is evidenced from the emission humps on either or both sides of the absorption core in Fig. 3 (also the white

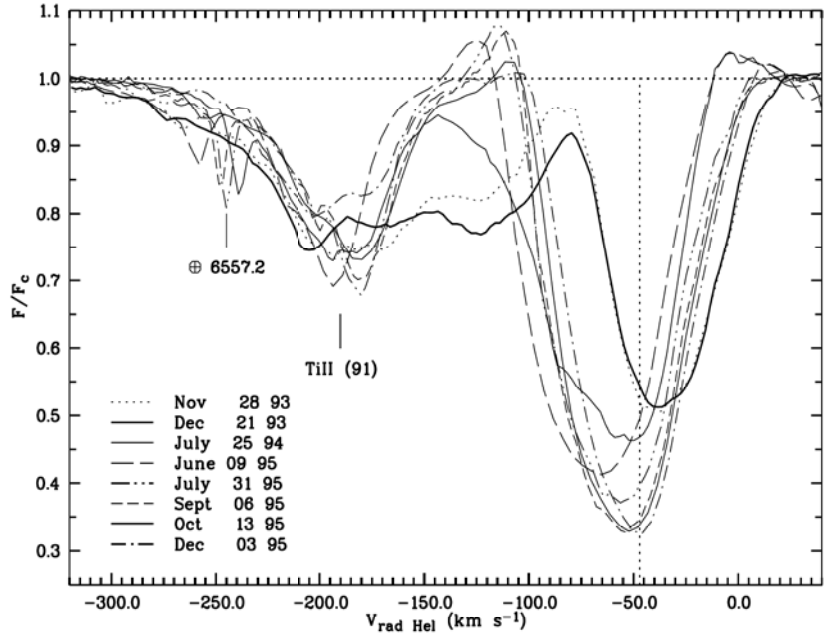

Figure 3. In contrast to the metallic lines, the Hα line core intensifies steadily over 24 months, while the line flanks turn mutually into emission. Notice the tremendous changes in the horizontally far blueward extended line wing over a period of only 24 days (Nov. 28-Dec. 21, 1993), whereas the line core remains static.

stripes in Fig. 5, left panel). We could not detect a velocity stratification from unsplit metallic absorption lines with 1 eV $< \chi_{\rm low} <$ 5 eV in our sequence of spectra. The amplitude of the latter lines remains below 15 km s^{-1}, whereas the Hα line core exceeds 35 km s^{-1} over the same period (Fig. 4). The intensity and radial velocity changes of the Hα line core appear in anti-phase with a much longer period, which might reflect a velocity stratification of the extended atmosphere of ρ Cas (Fig. 5) (for more details on the pulsation of ρ Cas see Lobel et al. 1998). The variability of Hα, which appears to be linked with the atmospherical pulsation, is however distorted by the clear filling-in by emission, presumably from a weak and varying quasi-chromosphere (de Jager et al. 1997).

4. The Emission Line Spectrum emerging from Bipolar Outflow

We have analyzed the emission line spectrum for three optical spectra of ρ Cas. We identified 11 prominent neutral emission lines in the spectrum of Dec. '93, when the overall absorption spectrum was weak. We have discovered two flat-

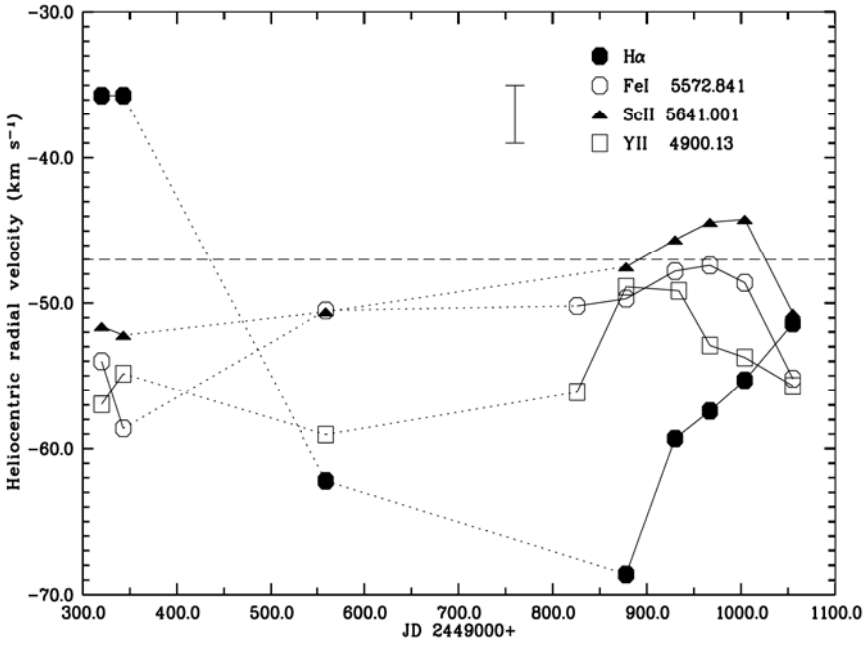

Figure 4. Heliocentric radial velocity changes of the Hα line core and of three metallic lines ($\chi_{\rm low}$ <3.4 eV) with respect to the stellar velocity (dashed drawn line)

topped [Ca II] lines, also observed in HR 8752, the spectroscopic twin of ρ Cas. These forbidden lines point to the presence of an optically thin and tenuous envelope surrounding the star, from which we can accurately determine the stellar center-of-mass velocity of -47 ± 2 km s^{-1}.

We have identified 30 split absorption lines of Fe I. The splitting of these line cores is linked with their low excitation energy, just like the prominent emission lines. The latter appear above the continuum level when the overall absorption spectrum is weak (the pulsation phase of high $T_{\rm eff}$).

Radial velocity measurements of the central reversals of the split profiles revealed that their velocities correspond with these of the prominent emission lines, as is shown in Fig. 6. Therefore, the split profiles are composed of a broad and deep absorption core formed in the pulsating photosphere, overlaid by a narrow and static emission line of the same atomic transition. The emission reversals have subsonic velocities close to the stellar velocity and appear to be steady during the photospherical oscillations. The absorption cores at either side of the central emission reversal are thus only apparently produced by the superposition spectrum and their intensities change oppositely due the pulsational Doppler shifts of the broad absorption line underneath (this spectral phenomenon can be viewed for a computed line in the MPEG movie on the CD

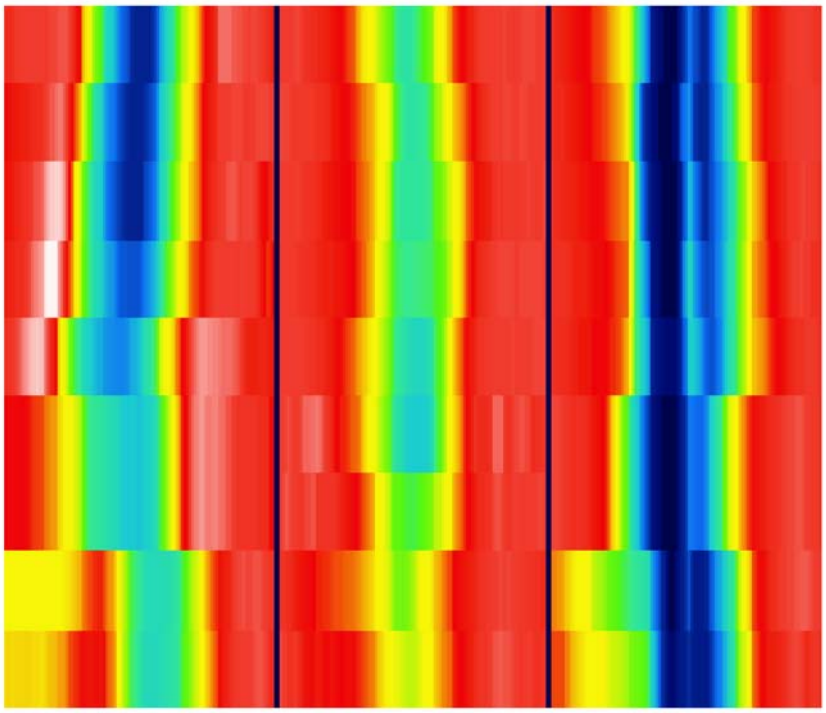

Figure 5. The three colored images display spectral changes of ρ Cas covering a period of about two years (time runs upward from Nov. '93 to Dec. '95). The red colored portions of the sequence correspond with the continuum level of the spectra. The other colors indicate the depression of light in three absorption lines; Hα, Fe I 5572 Å and Ba II 6141 Å (from left to right). The white stripes in Hα are emission. Notice the Doppler motion of the spectral lines with pulsation and the violet wing extensions of Nov.–Dec. '93. The Ba line core appears permanently split by a steady emission reversal. The heliocentric radial velocity scale on the abscissa ranges from –150 to 50 km s^{-1} (Lobel 1997)

ROM). High excitation absorption lines remain single and display large Doppler shifts with pulsation.

Next to this, we have measured the equivalent widths of 22 Fe I emission reversals for RMT 1, 15 and 36. For this purpose we find a best fit for the underlying absorption line onto the absorption flanks of the split profile. After subtracting from the observed profile we obtain an emission line which is fitted well by a Gaussian. From an application of the curve of growth method for the three multiplets we derive an excitation temperature of 3050 K for the emission line formation region (Lobel & de Jager 1997).

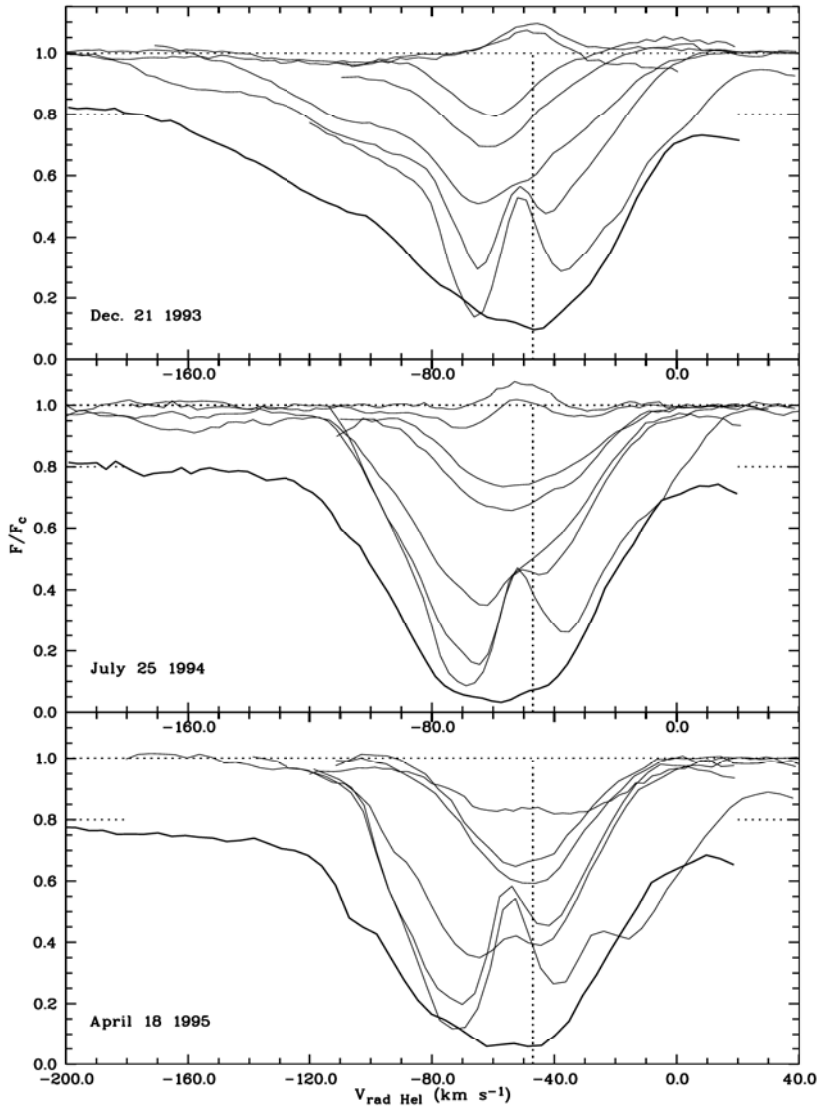

Figure 6. Comparison of prominent Fe I emission lines, two single absorption lines of high excitation energy and three split lines of RMT 15. The central reversals of the latter and the prominent emission lines are static and assume the same velocities, whereas the single absorption cores exhibit large Doppler shifts with the atmospherical pulsations. The lines with split cores can be fit into the broad core profile of Y II (thick drawn lines).

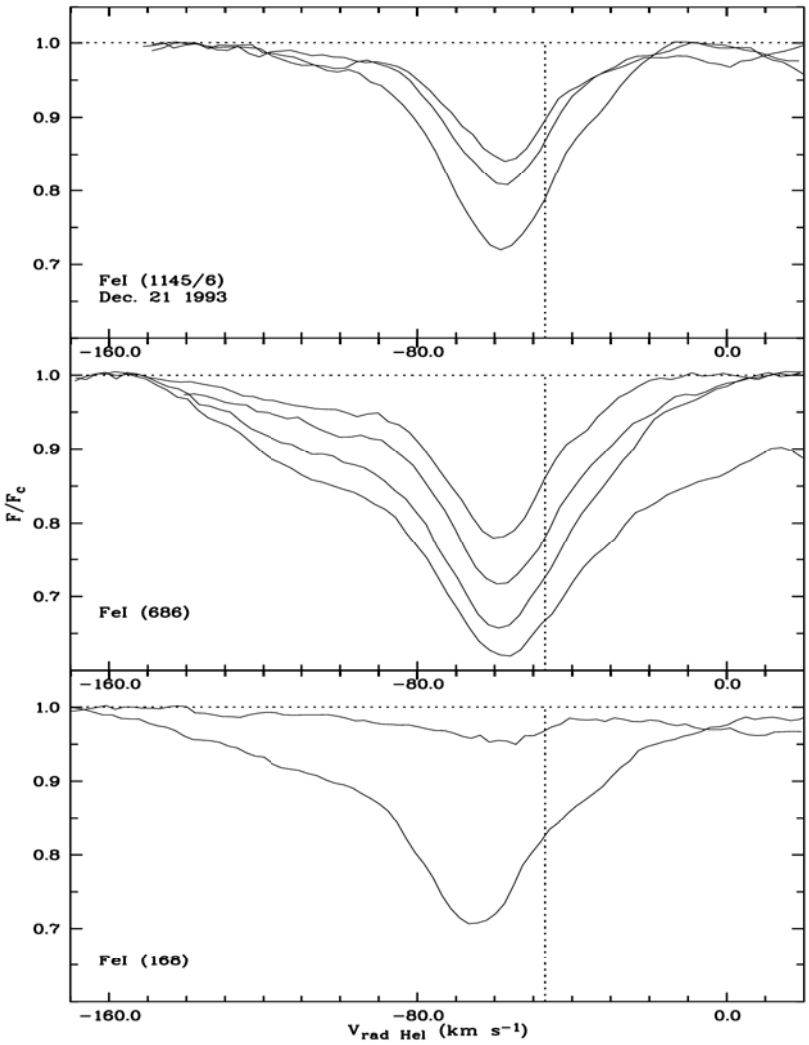

Figure 7. Nine unblended Fe I lines of Dec. 21 '93 from three multiplets. The $V_{\max}$ values measured in the extended violet wings increase with decreasing lower excitation energy.

The permanent asymmetric profile and blue-shifts by about the sound speed of these allowed emission lines has been modeled by a fast stellar wind collimated in two bipolar cones along a symmetry axis of outflow (for bipolar outflow detected in another cool hypergiant IRC+10420 see Humphreys et al. 1997). If LTE conditions can be maintained we calculate limited cone sizes being smaller or of the order of the stellar radius for opening angles $\alpha \geq 10^o$. An emission line formation region located that close to the stellar surface would be affected by the atmospherical pulsations. Since the emission spectrum is observed to be permanently static, its origin is therefore ascribed to two remote shells in the elongation of the bipolar cones, where the supersonic stellar wind is braking to subsonic values. From the classical Rankine-Hugoniot relations for a steady radiating shock wave we calculate shell distances to ρ Cas between 15 R_* and $\sim$150 R_* for $\alpha \geq 30^o$ (Lobel & de Jager 1997). Smaller opening angles of polar outflow provide distances which appear incompatible with the distance for dust formation as was estimated from *IRAS* infrared fluxes (Jura & Kleinmann 1990).

5. Turbulence, Mass Loss and Hα Emission by Stochastic Shocks in the Hypergiant ρ Cassiopeiae

We have tried to predict the $\dot{M}$, the microturbulent velocity component and the observed $H\alpha$ profile by assuming a stochastic field of shock waves in the atmosphere. It is known that hydrodynamical turbulence in a stellar atmosphere turns rapidly into a field of stochastic shock waves which are able to initiate a stellar wind and heat stellar atmospheric layers. Numerical calculations show (de Jager et al. 1997) that a maximum shock strength $M_{1,max} = 1.06$ to 1.08 appears to be fully capable of describing the observed rate of mass loss ($10^{-5} M_\odot$ yr^{-1}) and the supersonic value for the microturbulent velocity component (11–12 km s^{-1}). We find at the same time that the purely hydrodynamic component of shock-wave microturbulence is only $\sim$0.5 km s^{-1}, which is a much more reasonable value than the extreme values found when taking the spectral data at their face values. We suggest that the observed "microturbulent" line broadening is not caused by stochastic small-scale turbulent motions (the classical notion of microturbulence) but by the thermal motions in stochastically distributed high-temperature sheets behind the many shocks. We found that the accumulation of high-temperature sheets behind the many atmospheric shocks produces many relatively hot sheets, particularly in the outer layers of the star. In deeper layers shocks do not so much lead to the appearance of hot sheets because the shock heating is used for ionizing the atmosphere behind the shocks, with small or zero temperature enhancements. A non-LTE calculation of the expected profile of $H\alpha$ shows that a shocked atmosphere is indeed able to simulate the strongly variable displaced emission components. The variability of Hα is most probable linked with the atmospherical pulsation and distorted by a clear filling-in by emission, presumably from a weak and varying chromosphere.

6. The Stellar Wind

Our spectra of Dec. and Nov. '93 display the development of very far shortward extended wings in every photospheric absorption line. These spectra correspond to the pulsation phase near maximum $T_{\rm eff}$, while the extended wings disappear for low $T_{\rm eff}$, when the profiles become deep and center symmetrically around the stellar velocity (also Fig. 1). The shortward absorptions are produced in a supersonic wind for which we measure maximum outflow velocities of 150 km s^{-1} in Hα and velocities up to 130 km s^{-1} for metallic lines of very low excitation energy. A multiplet analysis of 9 unblended Fe I lines reveals $T_{\rm ex}$=2560 K in the supersonic wind. It corresponds with an upper value of the mass-loss rate near the phase of maximum $T_{\rm eff}$ of 9.2×10^{-5} M$_\odot$ y^{-1}. The velocity structure of the supersonic wind can be modeled by a β-power law. The latter is supported by our finding that the maximum velocities of the violet extended wings of Fe I tend to increase by $\sim$15 km s^{-1} per electron volt decline of the excitation energy (Fig. 7). We found that the mean formation region of these wings is located about $2.5\times R_*$ above the sonic point. The enhancement of the violet wings with the pulsation of the photosphere can be ascribed to two alternative mechanisms (Lobel et al. 1997). Either the supersonic wind is accelerated radiatively with the raise of $T_{\rm eff}$ in combination with an almost invariable mass-loss rate which maintains the extent of the wing formation region, or mechanical sources (see Nieuwenhuijzen & de Jager 1995) from the subsonic wind region modify the mass-loss rate drastically which alters the violet wing formation region and hence the observable wind velocities.

7. The Evolutionary Status

In our analysis of the Fe lines we obtained [Fe/H]=0.3±0.3. (Lobel et al. 1998; also Lobel et al. 1994 derived [Fe/H]=0.39±0.3 for the spectra of 1970). This slight overabundance with respect to the solar value can be partly due to the general increase (up to 0.2) in the metallicity of the Galaxy in the 4.6 Gyears of solar existence. The Na excess is due to the Ne-Na reaction cycle operating together with the C-N-O tri-cycle, while Na is brought to the photosphere by dredging-up. Oxygen is depleted as the result of deep mixing, in which the ashes of O $\rightarrow$ N burning and enhanced quantities of Na formed by proton captures on Ne, are convected into the atmosphere. We found that [Na/H]=0.65±0.15 which implies that ρ Cas is a post-red supergiant, evolving along the blueward loop in the HR-diagram. Given above range of [Na/H] implies a range of a current mass between 25–35 Our result is based on a LTE analysis of Na lines and can be overestimated due to non-LTE effects (Takeda & Takeda-Hidai 1994). However, note that the results of Takeda & Takeda-Hidai (1994) were based on another set of fundamental parameters of the star. Our results confirm once more the large abundance of Na mentioned already by Boyarchuk et. al (1988). In addition, a preliminary investigation of carbon lines shows that this element is underabundant and [C/H]$\sim -0.3 \pm 0.1$ (Israelian, de Jager & Lobel 1997). The difficulty with these carbon lines is that they are strongly blended and it is not clear how their formation is influenced by non-LTE effects. The α elements

Si, Mg, and Ca are essentially uniformly overabundant relative to their solar values on 0.3±0.1 dex.

References

de Jager, C. 1998, A&A Rev., 8, 145

de Jager, C., & Nieuwenhuijzen, H. 1997, MNRAS, 290, 50

de Jager, C., Lobel, A., & Israelian, G. 1997, A&A, 325, 714

Feast, M.W., & Tackeray, A.D. 1956, MNRAS116, 41

Humphreys, R.M., Smith, N., Davidson, K., Jones, T.J., Gehrz, R.D., Mason, C.G., Hayward, T.L., Houck, J.R., & Krautter, J. 1997, AJ, 114, 2778

Israelian, G., de Jager, C., & Lobel, A., 1997, in preparation

Jura, M., & Kleinmann, S.G. 1990, ApJ351, 583

Keenan, P.C. 1971, Contr. Kitt Peak Natl. Obs., 554, 35

Lobel, A., de Jager, C., Nieuwenhuijzen, H., Smolinski, J., & Gesicki, K. 1994, A&A, 291, 226

Lobel, A., Israelian, G., de Jager, C., Musaev, F., Parker, J.Wm., & Mavrogiorgou, A. 1998, A&A, 330, 659

Lobel, A. 1997, PhD Thesis, VU Brussels

Lobel, A., & de Jager, C., 1997, A&A, submitted

Nieuwenhuijzen, H., & de Jager, C. 1995, A&A, 302, 811

Takeda, Y., & Takada-Hidai, M. 1994, PASJ, 46, 395